Nonlinear calibration of a laser stripe profiler

Alan M. McIvor
Reveal Limited
P.O. Box 5907
Wellesley Street
Auckland, New Zealand
E-mail: alan.mcivor@reveal.co.nz

Abstract. The calibration of a laser stripe profiler consisting of a laser stripe projector, camera, and linear motion table is considered. A nonlinear system model is used, which accommodates radial distortion in the camera lens. The way in which stripe data is extracted from the camera images leads to a natural formulation of the calibration problem as a nonlinear least squares problem. This can then be solved using standard techniques. The use of this nonlinear model reduces the error in the generated 3-D data by over an order of magnitude. [DOI: 10.1117/1.1416694]

Subject terms: laser profiler; calibration; nonlinear methods; least squares.

Paper 200034 received Jan. 31, 2001; revised manuscript received June 25, 2001; accepted for publication June 28, 2001.

1 Introduction

A laser stripe profiler is one of many techniques[1] for generating dense 3-D surface information. Such data have uses in computer vision, computer graphics for generation of realistic object models, and medical applications.

A laser stripe profiler consists of a laser source, camera, and linear motion platform, in an arrangement such as illustrated in Fig. 1. The laser source emits a plane of light that forms an illuminated stripe on the object's surface. This is viewed by a camera displaced from the laser plane. In the indicated arrangement, the stripe runs roughly from the top to the bottom of the images. The horizontal displacement is related to surface shape. The data extracted from the image are in whichever column (x direction) the stripe crosses each row. The position in the x direction is estimated to subpixel accuracy using a subpixel operator such as Gaussian interpolation.[2] Given the camera intrinsic parameters and its relative location with respect to the laser plane, the position of the corresponding point in the laser stripe (i.e., the coordinates in the laser stripe plane) can be estimated by triangulation. Finally, these can be transformed into 3-D coordinates by incorporating the known motion of the object relative to the laser plane.

The classic approach to calibration of a laser striping system[3–6] is to first use a standard camera calibration technique, such as in Ref. 7, to estimate the camera parameters. Then the parameters of the laser plane are estimated by projecting observed points into 3-D locations and fitting a plane by least squares. This approach has a number of drawbacks. It divides the calibration into two subproblems, which may result in a suboptimal estimate of the parameters. More importantly, it requires an intensity image from the camera. In many systems, this is not feasible, because the camera lens may be heavily filtered so that only the laser light is visible, for example, or the images are processed on the fly within the sensor to extract stripe data and thus only stripe position data are available.

As noted before, part of the 3-D data generation procedure can be viewed as mapping observed image points to positions in the plane of the laser stripe. The latter is given by the distance from the camera optic center to the point in the laser stripe plane along the ray through the camera image point. It is commonly referred to as height and forms a 1-D function of the image coordinates. Estimating this function directly is the basis of several methods.

In Ref. 8, the height is assumed to be a cubic function of the image coordinates. A set of parallel planar surfaces (at different spacings off the motion table) are scanned. The parameters of the cubic are estimated from the known distance between the surfaces.

In Ref. 9, a more sophisticated calibration target is used, which has a staircase-like face. By scanning this, the height function is densely sampled. These data are used in a look-up table, along with linear interpolation, to approximate the height function on scanned objects. Height measurements are converted to 3-D coordinates by assuming that the height is in the Y-Z plane (i.e., this plane contains the laser source) and the motion is in the X-Y plane.

For these polynomial methods to generate accurate results, a complex calibration target is needed so that densely sampled data are generated. Better accuracy is obtained using a physical model of the system.[10]

In Ref. 11, a linear system model is used. A 3-D coordinate, $\mathbf{X}_l$, frame is associated with the laser plane (such that the laser lies in $x=0$). It is assumed that the transformation from this coordinate frame to a world coordinate frame, in which some calibration objects are measured, is known. Since the model is linear, the map from the image plane coordinates to a 2-D coordinate frame for the laser plane is specified by a 3×3 homotopy. By aligning the axes of the 2-D laser plane coordinates with the y and z axes of $\mathbf{X}_l$, a map can be defined from the image plane coordinates to $\mathbf{X}_l$. This is specified by a 4×3 matrix, of which the top row contains 0 (because of the choice that the laser lines on $x=0$) and the bottom three rows contain the homotopy from image plane to laser plane. The elements of this matrix can be estimated from the image plane locations of image points generated from several known world planes.

In Ref. 12, a nonlinear model of the system is used that incorporates standard terms in the camera model to handle

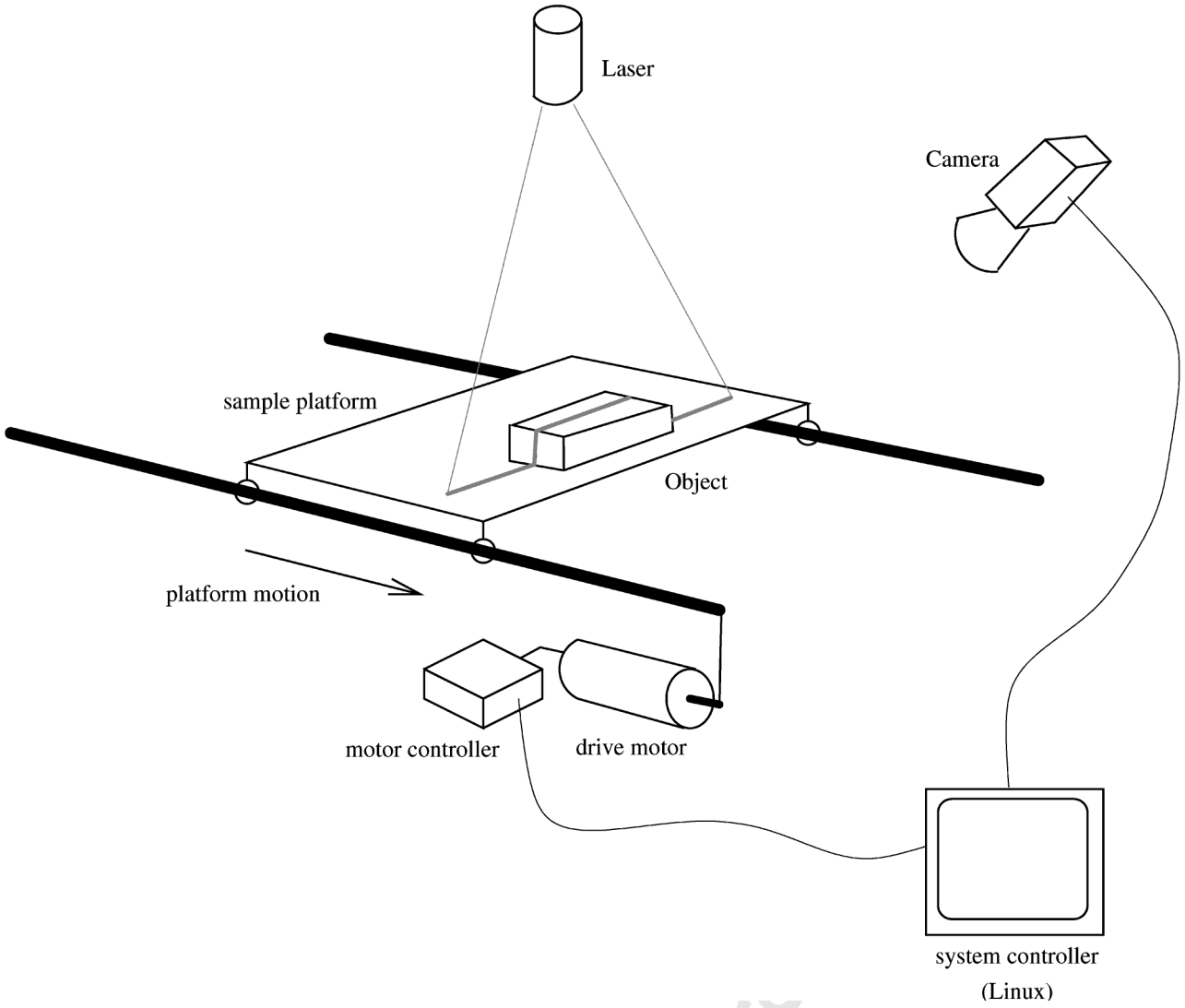

Fig. 1 Overview of the laser profiling system.

radial distortion effects. The raw data used are the motion platform position that particular points on a planar calibration target pass through the laser plane, and the observed image location. The points used are the centroids of circular disks on the surface. The required data have to be estimated by interpolation. The planar target is scanned in two different positions to generate enough data samples.

The method described resembles that in Ref. 11, in that the raw data observed from world planes are used in the calibration process. But unlike that work, a nonlinear system model is used. We use a nonlinear system model similar to that in Ref. 12. But it does not use fiducial marks as in Ref. 12, because this introduces the need to *a priori* interpolate sensor data. This combination of raw data as input and nonlinear system model results in improved accuracy. In many respects the approach taken here is similar to bundle adjustment procedures used in photogrammetry (e.g., Ref. 13) in that a nonlinear method is used to adjust the system parameters to best accommodate all measured data. The difference is that in this system, one of the components (the laser) is not a camera, although it can be considered in some respects to be a special type of linear camera. Another important contribution of this work is the formulation of the calibration as a nonlinear least squares problem, which means that standard numerical methods can be used to solve the problem.

The rest of this work is outlined as follows. In Sec. 2, the nonlinear system model is described. The details of the calibration procedure are presented in Sec. 3, and its experimental evaluation is described in Sec. 4. We conclude in Sec. 5 with a discussion of the method's performance and an indication of areas requiring further work.

2 System Description and Model

The laser stripe profiler consists of a camera viewing a scene into which a plane of laser light (generated with a cylindrical lens) is projected. The object of interest is moved through the scene along a linear trajectory. The camera and laser are arranged such that notionally the visible laser stripe appears as a vertical line in the camera's field of view, and such that the direction of motion is notionally along the camera/laser baseline. It is useful to iden-

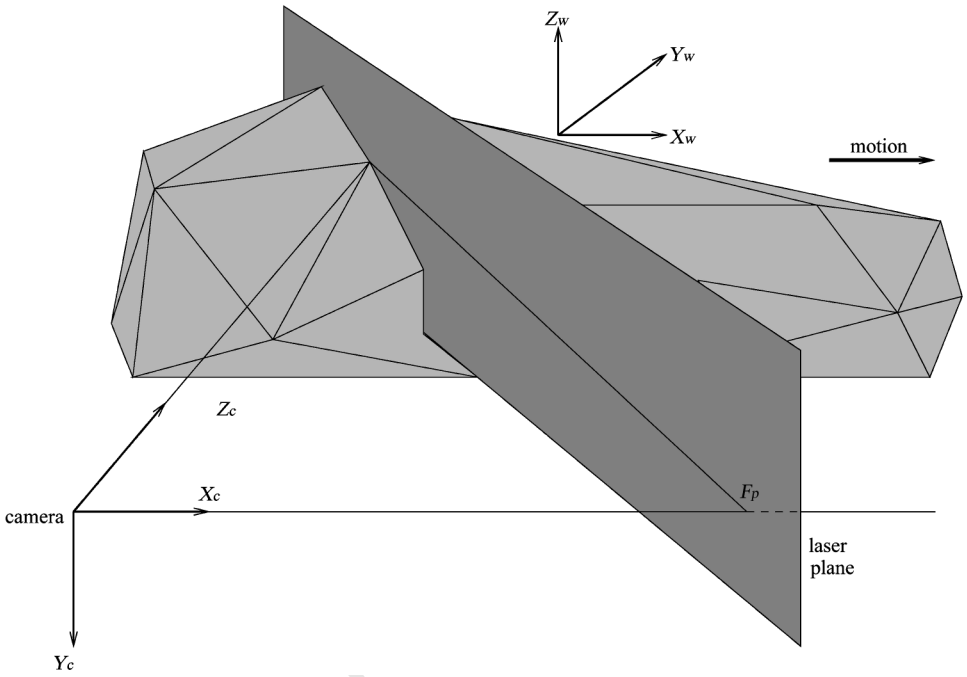

Fig. 2 3-D laser profiler model.

tify several coordinate frames as, shown in Fig. 2. The various coordinate frames will be identified with subscripts as follows:

- *w* world coordinate frame attached to object being measured (3-D)
- *c* camera coordinate frame (*i*3-D)
- *i* camera image plane coordinate frame (2-D).

Let $\mathbf{x}_w$ be the coordinates of a point on the surface of the object being profiled, in a world coordinate frame fixed relative to the object.

A coordinate frame $\mathbf{x}_c$ associated with the camera is introduced. The Euclidian transformation between the fixed and the camera coordinate frames is specified by a rotation $\mathbf{R}$ and a translation $\mathbf{t}$, namely

$$\mathbf{x}_c = \mathbf{R}\mathbf{x}_w + \mathbf{t} + t\Delta\mathbf{m}, \tag{1}$$

where t is the image number (starting at 0), i.e., the "time," Δ is the distance moved between images, and $\mathbf{m}$ is the unit vector representing the direction of travel between images.

A standard camera model containing a single nonlinear term for radial distortion is used.[13] The transformation from $\mathbf{x}_c$ to $\mathbf{x}_i$ is as follows. Let $\mathbf{x}_u$ be undistorted image plane coordinates given by

$$x_u = \frac{x_c}{z_c}, \quad y_u = \frac{y_c}{z_c}. \tag{2}$$

These are related to distorted image plane coordinates $\mathbf{x}_d$ by

$$\mathbf{x}_u = (1 + K_1 r^2)\mathbf{x}_d, \tag{3}$$

where $r^2 = x_d^2 + y_d^2$ and K_1 is a radial distortion coefficient. The observed image plane coordinates $\mathbf{x}_i$ are then

$$\mathbf{x}_i = \begin{bmatrix} s_x & k \\ 0 & s_y \end{bmatrix} \mathbf{x}_d + \begin{bmatrix} c_x \\ c_y \end{bmatrix}, \tag{4}$$

where s_x, s_y are focal lengths (measured in pixels) in each of the sensor grid directions, k is a skew parameter, and (c_x, c_y) is the optic center.

The light projected by the laser lies in a plane. The plane is specified by a normal $\mathbf{n}$ and an offset d from the origin. In the camera coordinate frame, the laser plane is thus represented by

$$\mathbf{n}_c^{\mathrm{T}} \mathbf{x}_c + d_c = 0. \tag{5}$$

Operation of the profiler generates $(\mathbf{x}_i, t)$ tuples for points on the surfaces of visible objects. From these, an estimate of $\mathbf{x}_w$ is to be generated. From Eq. (4),

$$\mathbf{x}_d = \begin{bmatrix} \frac{1}{s_x} & \frac{-k}{s_x s_y} \\ 0 & \frac{1}{s_y} \end{bmatrix} \left(\mathbf{x}_i - \begin{bmatrix} c_x \\ c_y \end{bmatrix} \right). \tag{6}$$

Hence $\mathbf{x}_u$ can be calculated from Eq. (3), and $\mathbf{x}_c$ expressed as

$$\mathbf{x}_c = z_c \begin{bmatrix} \mathbf{x}_u \\ 1 \end{bmatrix} \tag{7}$$

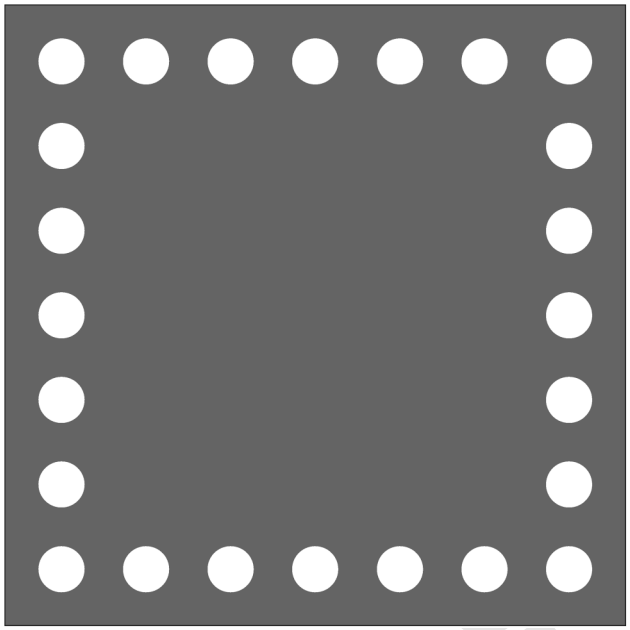

Fig. 3 The pattern used on each face of the calibration target.

in terms of the unknown z_c. Substituting this into Eq. (5), we obtain

$$z_c = \frac{-d_c}{\mathbf{n}_c^{\mathrm{T}} \begin{bmatrix} \mathbf{x}_u \\ 1 \end{bmatrix}}. \tag{8}$$

Thus, $\mathbf{x}_w$ can be determined from Eq. (1).

3 System Calibration

Calibration is the determination of optimal values for the model parameters: $\mathbf{R}$, $\mathbf{t}$, $\mathbf{m}$, $\mathbf{n}_c$, d_c, s_x, k, c_x, s_y, c_y, and K_1. This is accomplished by scanning a calibration target about which world information is *a priori* known. The target used consists of several planar surfaces having the pattern shown in Fig. 3 printed on them. A three surface target is shown in Fig. 4. The data obtained from scanning the calibration target are presented to an operator as the intensity recorded along the laser stripe for each scan, as shown in Fig. 5. The operator then identifies the regions corresponding to the circular fiducial marks and the rectangular planar regions. These data are used in the parameter estimation process.

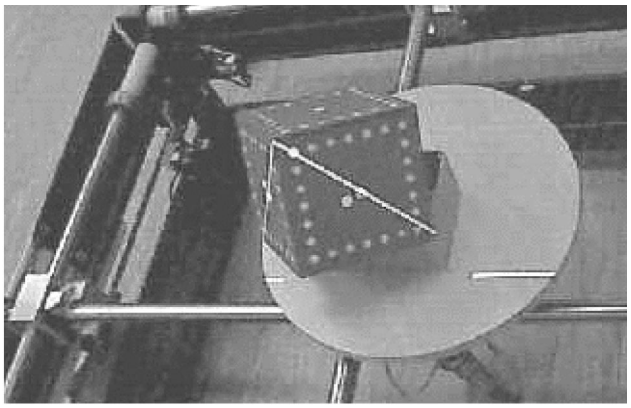

Fig. 4 A calibration target consisting of three planar faces.

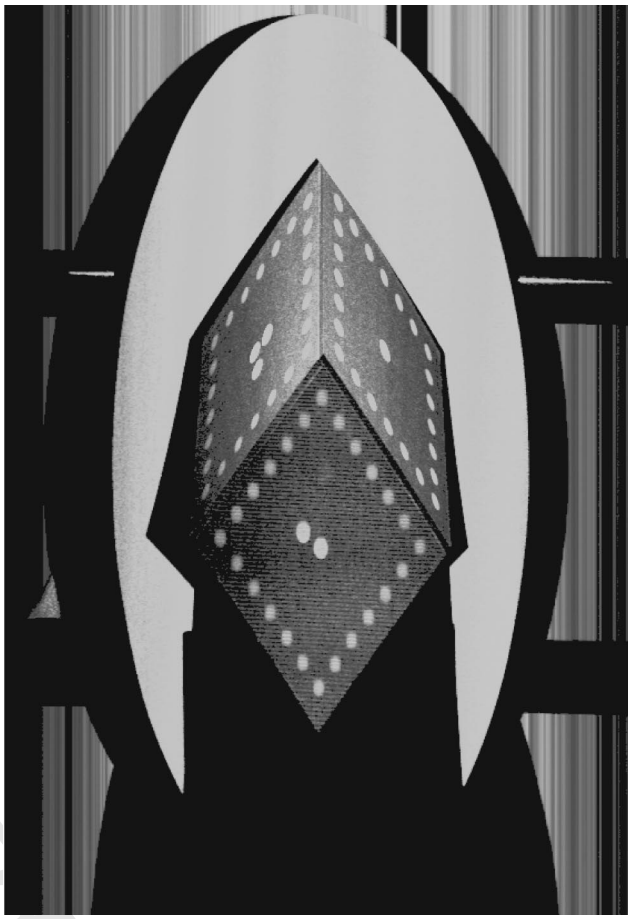

Fig. 5 Image constructed from intensity recorded along the laser stripe in each scan.

Determining optimal values for the model parameters can be formulated as a nonlinear regression problem, as shown in Sec. 3.1. This uses the raw scan data from the planar surfaces only. The nonlinear regression problem can be solved using any one of a variety of standard numerical tools. Most of these methods only guarantee to find values that are locally optimal, and need some form of augmentation to maximize the likelihood of finding the global optimum. One approach would be to use a generic strategy, such as starting the numerical method from several random sets of initial parameter estimates. However, a good initial estimate is easily obtained by ignoring the radial distortion parameter, i.e., assuming $K_1 = 0$. By doing so, the problem of estimating the remaining parameters can be converted into a linear function of the 3-D coordinates of the fiducial marks, and the position/time when they are observed to pass through the laser stripe. This procedure is described in Sec. 3.2. The position and time when a fiducial mark passes through a stripe is not directly measured, but needs to be estimated from the raw data. A method for doing this is given in Sec. 6.

3.1 *Nonlinear Estimation*

The planar surfaces of the calibration target are specified in a world coordinate frame associated with the target as

$$\mathbf{p}_w(k)^{\mathsf{T}}\mathbf{x}_w + q_w(k) = 0, \quad k = 1 \ldots N. \tag{9}$$

An external measurement system is required to provide the calibration target parameters

$$\mathbf{p}_w(k), q_w(k), k = 1, \ldots, N.$$

The raw data acquired from the target consists of sets of tuples (x_i, y_i, t) for each plane k, which record when the stripe at time t lies on plane k, such that the stripe is measured to intersect row y_i at column x_i^o. Thus, if φ represents the system parameters ($\mathbf{R}$, $\mathbf{t}$, s_x, etc.), and the system model can be expressed as

$$x_i = f_k(y_i, t; \varphi), \tag{10}$$

then the system parameters can be estimated by nonlinear least squares minimization of

$$E = \sum_k \sum_{y_i} [x_i^o - f_k(y_i, t; \varphi)]^2. \tag{11}$$

The rest of this section shows how f_k can be derived. The k'th calibration target plane in Eq. (9) can be expressed in camera coordinates as

$$\mathbf{p}_c^{\mathsf{T}}\mathbf{x}_c + q_c = 0, \tag{12}$$

where the k arguments have been dropped for clarity, and

$$\mathbf{p}_c = \mathbf{R}\mathbf{p}_w(k) \tag{13}$$

$$q_c = q_w(k) + t\Delta\mathbf{p}_w(k)^{\mathsf{T}}\mathbf{m} - \mathbf{p}_c^{\mathsf{T}}\mathbf{t}. \tag{14}$$

Hence Eq. (8) can be rewritten as

$$z_c = \frac{-d_c}{(n_1 x_d + n_2 y_d)(1 + K_1 r^2) + n_3}, \tag{15}$$

where the n_i are the components of $\mathbf{n}_c$. Substituting this into Eq. (12) gives

$$(1 + K_1 r^2)[q_c(n_1 x_d + n_2 y_d) - d_c(p_1 x_d + p_2 y_d)] + q_c n_3 - d_c p_3 = 0, \tag{16}$$

where the p_i are the components of $\mathbf{p}_c$. Substituting for r, x_d, and y_d from Eq. (6) gives a cubic polynomial for x_i in terms of t, y_i, the system parameters, and the calibration target plane parameters:

$$Ax_i^3 + Bx_i^2 + Cx_i + D = 0, \tag{17}$$

where

$$A = K_1\beta^3\alpha_1 \tag{18}$$

$$B = K_1\beta^2(3\alpha_1\gamma + \alpha_2 y_d) \tag{19}$$

$$C = \beta\alpha_1 + K_1\beta(\alpha_1 y_d^2 + 2\alpha_2\gamma y_d + 3\alpha_1\gamma^2) \tag{20}$$

$$D = \alpha_3 + \alpha_1\gamma + \alpha_2 y_d + K_1(\alpha_2 y_d + \alpha_1\gamma)(y_d^2 + \gamma^2) \tag{21}$$

$$\alpha = q_c\mathbf{n}_c - d_c\mathbf{p}_c \tag{22}$$

$$\beta = \frac{1}{s_x} \tag{23}$$

$$\gamma = -\beta(k y_d + c_x) \tag{24}$$

$$y_d = \frac{y_i - c_y}{s_y}. \tag{25}$$

3.2 *Initial Parameter Estimation*

By assuming that $K_1 = 0$ (so that $\mathbf{x}_d = \mathbf{x}_u$), the camera model in Eqs. (1) through (4) can be written succinctly in homogeneous coordinates as

$$\begin{bmatrix}\mathbf{x}_i \\ 1\end{bmatrix} = \lambda\mathbf{K}[\mathbf{R} \quad \mathbf{t} + t\Delta\mathbf{m}]\begin{bmatrix}\mathbf{x}_w \\ 1\end{bmatrix}, \tag{26}$$

where

$$\mathbf{K} = \begin{bmatrix} s_x & k & c_x \\ 0 & s_y & c_y \\ 0 & 0 & 1 \end{bmatrix}. \tag{27}$$

By subtracting the third row multiplied by x_i from the first, and the third row multiplied by y_i from the second, Eq. (26) is reduced to two equations that do not contain λ. These can be rearranged into

$$\begin{bmatrix} x_w & y_w & z_w & 1 & 0 & 0 & 0 & 0 & -x_i x_w & -x_i y_w & -x_i z_w & -x_i & t\Delta & 0 & -t\Delta x_i \\ 0 & 0 & 0 & 0 & x_w & y_w & z_w & 1 & -y_i x_w & -y_i y_w & -y_i z_w & -y_i & 0 & t\Delta & -t\Delta y_i \end{bmatrix}\mathbf{l}_1 = 0, \tag{28}$$

where

$$\mathbf{l}_1 = [\mathbf{K}_1\mathbf{R} \quad \mathbf{K}_1\mathbf{t} \quad \mathbf{K}_2\mathbf{R} \quad \mathbf{K}_2\mathbf{t} \quad \mathbf{K}_3\mathbf{R} \quad \mathbf{K}_3\mathbf{t} \quad \mathbf{K}_1\mathbf{m} \quad \mathbf{K}_2\mathbf{m} \quad \mathbf{K}_3\mathbf{m}]^{\mathsf{T}}, \tag{29}$$

using the notation $\mathbf{K}_j$ for the j'th row of $\mathbf{K}$. This collects all of the involved unknown system parameters into $\mathbf{l}_1$.

The laser plane equation (5) can be transformed into world coordinates to give

$$\mathbf{n}_c^T\mathbf{R}\mathbf{x}_w+\mathbf{n}_c^T\mathbf{t}+t\Delta\mathbf{n}_c^T\mathbf{m}+d_c=0. \tag{30}$$

This can be written as

$$[x_w \quad y_w \quad z_w \quad 1 \quad t\Delta]\mathbf{l}_2=0, \tag{31}$$

where

$$\mathbf{l}_2=[\mathbf{n}_c^T\mathbf{R} \quad \mathbf{n}_c^T\mathbf{t}+d_c \quad \mathbf{n}_c^T\mathbf{m}]^T. \tag{32}$$

If the internal structure of $\mathbf{l}_1$ and $\mathbf{l}_2$ is ignored and instead they are treated as independent vectors, then Eqs. (28) and (31) form constraints to solve $\mathbf{l}_1$ and $\mathbf{l}_2$ separately. The next two subsections show how this can be done using linear methods. The final step is to estimate the original parameters from $\mathbf{l}_1$ and $\mathbf{l}_2$. Standard QR decomposition techniques, e.g., Ref. 14, are available that decompose $\mathbf{l}_1$ into the camera extrinsic parameters $\mathbf{R}$ and $\mathbf{t}$, and the camera intrinsic parameters s_x, s_y, k, c_x, and c_y, and to recover $\mathbf{n}_c$ and d_c. The remaining system parameter is the motion direction $\mathbf{m}$, which can be estimated from $\mathbf{l}_2$ using the pseudo-inverse.

3.2.1 *Camera parameters*

Let $\mathbf{A}_1$ be the $2N\times 15$ matrix formed by stacking Eq. (28) for each of the available data points one above the other, given that there are N fiducial marks. Thus, the estimate for the parameters $\mathbf{l}_1$ is the solution to

$$\min_{\mathbf{l}_1}\|\mathbf{A}_1\mathbf{l}_1\|^2, \tag{33}$$

subject to a constraint, say $\|\mathbf{l}_1\|=1$, to avoid the trivial solution $\mathbf{l}_1=0$. The estimate of $\mathbf{l}_1$ is then the singular vector associated with the smallest singular value of $\mathbf{A}_1$.[15]

3.2.2 *Laser stripe parameters*

Let $\mathbf{A}_2$ be the $N\times 5$ matrix formed by stacking Eq. (31) for each of the available data points one above the other. Thus, the estimate for the parameters $\mathbf{l}_2$ is the solution to

$$\min_{\mathbf{l}_2}\|\mathbf{A}_2\mathbf{l}_2\|^2, \tag{34}$$

subject to a constraint to avoid the trivial solution $\mathbf{l}_2=0$. The most natural constraint to impose is that the sum of squares for the first three components of $\mathbf{l}_2$ equal 1, since these represent the unit vector $\mathbf{n}_f$. If we define

$$\mathbf{B}=\begin{bmatrix}\mathbf{I}_3 & 0\\ 0 & 0\end{bmatrix}, \tag{35}$$

then the estimate of $\mathbf{l}_2$ is the solution to

$$\min_{\mathbf{l}_2}\|\mathbf{A}_2\mathbf{l}_2\|^2 \text{ subject to } \|\mathbf{B}\mathbf{l}_2\|^2=1. \tag{36}$$

This is a constrained minimization of a quadratic form with quadratic constraints and has a solution as follows. Let

$$\mathbf{l}_{21}=[n_1 \quad n_2 \quad n_3]^T \tag{37}$$

$$\mathbf{l}_{22}=[d \quad a_4]^T, \tag{38}$$

so that $\mathbf{l}_2=[\mathbf{l}_{21} \quad \mathbf{l}_{22}]^T$. Let $\mathbf{A}_{21}$ be the first three columns of $\mathbf{A}_2$ and let $\mathbf{A}_{22}$ be the last two columns. Define

$$\mathbf{C}=\mathbf{A}_{21}^T(\mathbf{I}_N-\mathbf{A}_{22}(\mathbf{A}_{22}^T\mathbf{A}_{22})^{-1}\mathbf{A}_{22}^T)\mathbf{A}_{21}, \tag{39}$$

then $\mathbf{l}_{21}$ is the eigenvector of $\mathbf{C}$ associated with the smallest eigenvalue of $\mathbf{C}$, and $\mathbf{l}_{22}$ is given by

$$\mathbf{l}_{22}=-(\mathbf{A}_{22}^T\mathbf{A}_{22})^{-1}\mathbf{A}_{22}^T\mathbf{A}_{21}\mathbf{l}_{21}. \tag{40}$$

4 Experimental Results

An experimental system was constructed to test this algorithm. It consisted of a linear motion platform that moved in a horizontal plane. A class C red laser with a Gaussian lens was used to generate a vertical laser plane such that the direction of platform motion was perpendicular to the laser plane. The motion platform moved 600 mm during scanning, starting 300 mm to one side of the laser plane. A standard 1/3-in. CCIR CCD camera was used to capture images via a 4.8-mm lens. It was positioned above the motion platform looking down 45 deg toward where the laser plane intersected the plane in which the linear motion platform moved, and approximately 1200 mm from that point. The motion platform was moved 0.5 mm between scans. Note that the measurements given are nominal values. The components were not carefully arranged to be at these positions. The exact positioning is unknown. The CCIR video signal was digitized with a Matrox Meteor framegrabber at 576×768 resolution. Images were captured in a darkened room to enhance the contrast.

The method was applied to data from the test system. Typical results from the linear initial parameter estimation scheme are

$$\mathbf{n}_c^T=[0.000 \quad -0.000 \quad -0.999] \tag{41}$$

$$d_c=-0.313 \tag{42}$$

$$\mathbf{m}^T=[0.005 \quad 0.113 \quad -0.993] \tag{43}$$

$$\mathbf{R}=\begin{bmatrix}-0.807 & -0.412 & -0.422\\ -0.019 & -0.697 & 0.717\\ -0.590 & 0.587 & 0.554\end{bmatrix} \tag{44}$$

$$\mathbf{t}^T=[0.070 \quad -0.001 \quad -0.156] \tag{45}$$

$$s_x,k,c_x,s_y,c_y,K_1=1.09,0.009,255.1,1.505,292.8,0.0 \tag{46}$$

$$\text{rms}(E)=0.04264, \tag{47}$$

Table 1 Statistics for distance from plane for back-projecting observed $(\mathbf{x}_i, t)$ data into 3-D and measuring distance from true planes.

	Mean (m)	Std Dev (m)
Linear	−0.031392	0.032319
Nonlinear	0.000016	0.001140

where the distance units are meters. The last item rms(E) is calculated by dividing the value of Eq. (11) by the number of data points and taking the square root of this.

The nonlinear least squares problem in Eq. (11) was solved using the Polak-Ribiere conjugate gradient method.[16] The output of the nonlinear estimation from this starting point generated the following results

$$\mathbf{n}_c^{\mathsf{T}} = [0.820 \quad 0.071 \quad 0.574] \tag{48}$$

$$d_c = -0.466 \tag{49}$$

$$\mathbf{m}^{\mathsf{T}} = [0.868 \quad -0.304 \quad 0.390] \tag{50}$$

$$\mathbf{R} = \begin{bmatrix} -0.867 & 0.335 & 0.368 \\ 0.054 & -0.672 & 0.738 \\ 0.495 & 0.670 & 0.565 \end{bmatrix} \tag{51}$$

$$\mathbf{t}^{\mathsf{T}} = [-0.191 \quad 0.039 \quad 0.833] \tag{52}$$

$$s_x, k, c_x, s_y, c_y, K_1 = 1000.0, -0.00004, 256.0, 1000, 256.0, -0.0014 \tag{53}$$

$$\text{rms}(E) = 0.001453. \tag{54}$$

This shows an order of magnitude improvement in the rms error.

Another measure of the performance is to back-project each observation point $(\mathbf{x}_i, t)$ into 3-D and measure the distance from the true plane that the data point lies on. Statistics of these are given in Table 1 and show an order of magnitude improvement in standard deviation.

The back-projected data points using the parameters resulting from the nonlinear estimation are illustrated in Fig. 6.

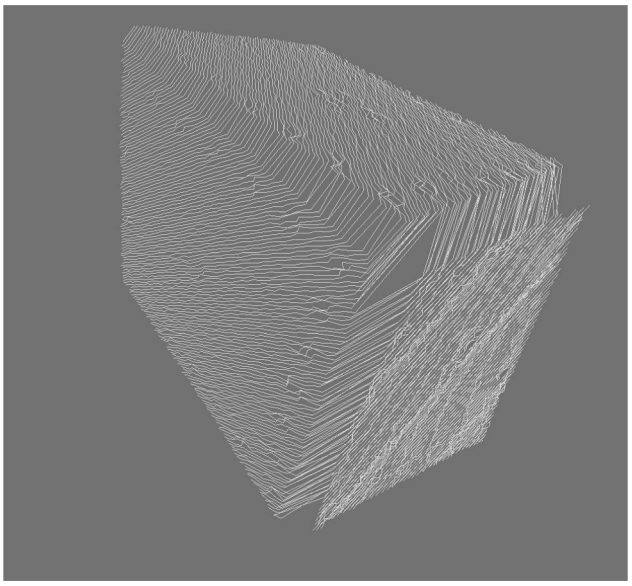

Fig. 6 Calibration target 3-D data reconstructed using the parameters from the nonlinear estimator.

5 Conclusion

A nonlinear least-squares-based method for calibrating a laser stripe profiling system is presented. A nonlinear model of the system is used, which allows for radial distortion in the camera lens. A calibration target consisting of a set of planar surfaces is used. An explicit function for the error in the stripe observations off this target is developed. This is then used in a nonlinear least squares algorithm. A separate linear calibration method is used to generate initial estimates of the system parameters. The nonlinear estimation method results in a significant improvement in the system's performance.

A number of areas have been identified for future work. The use of centroid estimates in the preliminary calibration phase is a major source of errors. They will be replaced with corner features, and ultimately, a linear calibration method that uses the same raw data as the nonlinear phase. Another useful step will be to incorporate the relative position of the planar faces into the set of unknown system parameters, which will mean that an expensive calibration target will be unnecessary. The extension of the technique to using an arbitrary surface via ray tracing will also be investigated.

6 Appendix: Fiducial Mark Estimation

The fiducial marks used in this initialization phase are the white disks on the targets. The required data are, for each fiducial mark j, the image plane location and time $[x_i(j), y_i(j), t_i(j)]$ when the fiducial mark's centroid passes through the laser plane. By using a centroid operator, this can be estimated from the observed data $[x_i(y_i,t) y_i]^{\mathsf{T}}$, where the image of the laser stripe intersects image row $y_i = 0 \ldots N$ at sample times $t = 0 \ldots T$, and the image intensity $I(y_i, t)$ at that stripe location. Let $\mathcal{N}(j)$ be the set of all data triples $[x_i(y_i,t), y_i, t]$ identified to be in the vicinity of fiducial mark j, such that $I(y_i,t) > \tau$. Then the estimate of the fiducial mark position is given by

$$\tilde{x}_i(j) = \frac{\Sigma_{[x_i(y_i,t),y_i,t]\in\mathcal{N}(j)} I(y_i,t) x_i(y_i,t)}{\Sigma_{[x_i(y_i,t),y_i,t]\in\mathcal{N}(j)} I(y_i,t)} \tag{55}$$

$$\tilde{y}_i(j) = \frac{\Sigma_{[x_i(y_i,t),y_i,t]\in\mathcal{N}(j)} I(y_i,t) y_i}{\Sigma_{[x_i(y_i,t),y_i,t]\in\mathcal{N}(j)} I(y_i,t)} \tag{56}$$

$$\tilde{t}(j) = \frac{\Sigma_{[x_i(y_i,t),y_i,t]\in\mathcal{N}(j)} I(y_i,t) t}{\Sigma_{[x_i(y_i,t),y_i,t]\in\mathcal{N}(j)} I(y_i,t)}. \tag{57}$$

In practice, $\mathcal{N}(j)$ is identified as follows in an interactive manner. The user is shown an image in which each row

shows the intensity recorded along the laser stripe for a particular scan, and the scans are stacked one above another to form the columns, as shown in Fig. 5. The operator identifies the location of several such points, so that an approximate estimate of the calibration parameters can be generated. This is used to project all of the fiducial marks onto the image. Then all image points that are within a elliptic region centered on these estimates and having an intensity larger than the threshold τ form $\mathcal{N}(j)$.

Acknowledgments

This work was funded by the New Zealand Foundation for Research, Science, and Technology as part of the ''3D Vision'' project within Contract CO8806 Objective 1 ''Machine Vision Techniques'' while the author was employed by Industrial Research Limited, P.O. Box 2225, Auckland, New Zealand.

References

1. R. Jarvis, ''Range sensing for computer vision,'' in *Three-Dimensional Object Recognition Systems*, Vol. 1 of *Advances in Image Communications*, A. K. Jain and P. J. Flynn, Eds., pp. 17–56, Elsevier Science Publishers, Amsterdam (1993).
2. D. K. Naidu and R. B. Fisher, ''A comparative analysis of algorithms for determining the peak position of a stripe to sub-pixel accuracy,'' in *British Machine Vision Conference*, P. Mowforth, Ed., pp. 217–225, Univ. Glasgow, Springer, Berlin (Sept. 1991).
3. R. C. Bolles, J. H. Kremers, and R. A. Cain, ''A simple sensor to gather three-dimensional data,'' Technical report 249, SRI, Stanford Univ. (1981).
4. C. H. Chen and A. C. Kak, ''Modelling and calibration of a structured light scanner for 3D robot vision,'' *IEEE Conf. Robotics Automation*, pp. 807–815 (1987).
5. M. Chiarella and K. A. Pietrzak, ''An accurate calibration technique for 3-D laser stripe sensors,'' *Proc. SPIE* **1194**, 176–185 (1989).
6. T. Pajdla, ''Laser plane range finder: The implementation at the CVL,'' Research report K335-1995-98, Computer Vision Laboratory, Czech Technical Univ., CZ-121 35 Praha 2, Karlovo nam. 13 (Oct 1995).
7. R. Y. Tsai, ''An efficient and accurate camera calibration technique for 3-D machine vision,'' *IEEE Conf. Computer Vis. Patt. Recog.*, pp. 364–374 (June 1986).
8. F. W. DePiero and M. M. Trivedi, ''3-D computer vision using structured light: Design, calibration and implementation issues,'' *Adv. Computers* **43**, 243–278 (1995).
9. E. Trucco, R. B. Fisher, and A. W. Fitzgibbon, ''Direct calibration and data consistency in 3-D laser scanning,'' in *BMVC94: Proc. 5th British Mach. Vis. Conf.*, Edwin Hancock, Ed., pp. 489–498, BMVA Press, Sheffield (Sept 1994).
10. C. Brenner, J. Bohm, and J. Guhring, ''Photogrammetric calibration and accuracy evaluation of a cross-pattern stripe projector,'' *Proc. SPIE* **3641**, 164–172 (1999).
11. I. D. Reid, ''Projective calibration of a laser-stripe range finder,'' *Image Vis. Comput.* **14**(9), 659–666 (Oct. 1996).
12. B. Tiddeman, N. Duffy, G. Rabey, and J. Lokier, ''Laser-video scanner calibration without the use of a frame store,'' *IEE Proc. Vision Image Signal Process.* **145**(4), 244–248 (1998).
13. *Manual of Photogrammetry*, C. C. Slama, Ed., American Society of Photogrammetry (1980).
14. R. I.Hartley; and P. Sturm, ''Triangulation,'' *Computer Vis. Image Underst.* **68**(2), 146–157 (Nov 1997).
15. A. M. McIvor and R. J. Valkenburg, ''Calibrating a structured light system,'' in *Image & Vision Computing New Zealand*, pp. 167–172, Industrial Research Limited, Lincoln, Canterbury (Aug 1995).
16. W. Press, S. Teukolsky, W. Vetterling, and B. Flannery, *Numerical Recipes in C*, Cambridge Univ. Press, Boston, MA (1988).

Alan McIvor is a research engineer with a strong interest in computer vision. Currently he works for Reveal Ltd., where he leads the development of a visual surveillance system used for providing pedestrian information in retail, casino, and shopping mall type situations. Prior to 2000 he spent six years at Industrial Research Ltd., where his interests were in the interpretation of data from 3-D scanners. He has also worked for British Petroleum on image processing systems for subsea vehicle control and at the Oxford University Robotics Research Group on autonomous vehicle guidance systems. He was granted a PhD in engineering from Harvard University in 1986 and a BE in engineering science from Auckland University.